Simultaneous Hydrogen Generation and Waste Acid Neutralization in a Reverse Electrodialysis System

3 AUTHORS:

Marta Hatzell
Georgia Institute of Technology
27 PUBLICATIONS **350** CITATIONS

SEE PROFILE

X.P. Zhu
Pennsylvania State University
35 PUBLICATIONS **885** CITATIONS

SEE PROFILE

Bruce E Logan
Pennsylvania State University
**458** PUBLICATIONS **33,239** CITATIONS

SEE PROFILE

Simultaneous Hydrogen Generation and Waste Acid Neutralization in a Reverse Electrodialysis System

Marta C. Hatzell,[†] Xiuping Zhu,[‡] and Bruce E. Logan*,[‡]

[†]Department of Mechanical and Nuclear Engineering and [‡]Department of Civil and Environmental Engineering, 212 Sackett Building, The Pennsylvania State University, University Park, Pennsylvania 16802, United States

S *Supporting Information*

ABSTRACT: Waste acid streams produced at industrial sites are often co-located with large sources of waste heat (e.g., industrial exhaust gases, cooling water, and heated equipment). Reverse electrodialysis (RED) systems can be used to generate electrical power and hydrogen gas using waste heat-derived solutions, but high electrode overpotentials limit system performance. We show here that an ammonium bicarbonate (AmB) RED system can achieve simultaneous waste acid neutralization and *in situ* hydrogen production, while capturing energy from excess waste heat. The rate of acid neutralization was dependent on stack flow rate and increased 50× (from 0.06 ± 0.04 to 3.0 ± 0.32 pH units min^{-1} m^{-2} membrane), as the flow rate increased 6× (from 100 to 600 mL min^{-1}). Acid neutralization primarily took place due to ammonium electromigration ($37 \pm 4\%$) and proton diffusion ($60 \pm 5\%$). The use of a synthetic waste acid stream as a catholyte (pH ≈ 2) also increased hydrogen production rates by 65% (from 5.3 ± 0.5 to 8.7 ± 0.1 m^3 H$_2$ m^{-3} catholyte day^{-1}) compared to an AmB electrolyte (pH ≈ 8.5). These findings highlight the potential use of dissimilar electrolytes (e.g., basic anolyte and acidic catholyte) for enhanced power and hydrogen production in RED stacks.

KEYWORDS: *Reverse electrodialysis, Ammonium bicarbonate, Hydrogen evolution reaction, Waste acid neutralization*
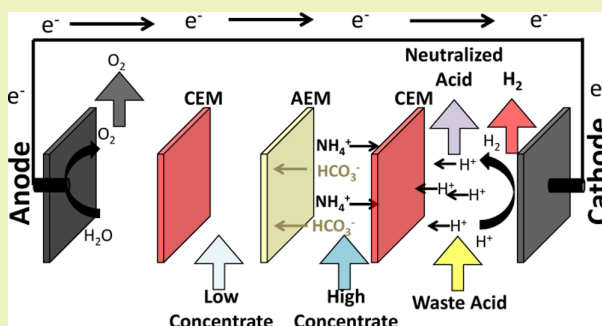
■ INTRODUCTION

Energy recovery during waste disposal is growing in importance at industrial sites.[1,2] Current industrial pollution control practices used to treat waste acids are based on pH neutralization, which requires mixing the acid with a basic or salt solution (carbonate or bicarbonate) and generates heat. Capture of this wasted energy, in a useable form (electricity or hydrogen), would help offset treatment costs and avoid energy consumption for pollution control. One recently proposed method to recover energy during treatment was based on harvesting mechanical energy during neutralization by repeatedly shrinking and swelling an ion-exchange resin in a waste acid or base solution, but energy yields were low.[3−5] Another approach was based on using the waste acid and base in an electrodialysis (ED) stack to desalinate water, but this water may not be desirable at many locations. A new approach is proposed here based on using the waste acid stream for improved energy production in a closed loop ammonium bicarbonate (AmB)-based reverse electrodialysis (RED) system.

RED is a salinity gradient energy (SGE) technology that can generate electricity through the controlled mixing of two bodies of water with different salt concentrations.[6−10] A RED system consists of a series of alternating anion (AEMs) and cation exchange membranes (CEMs), which drive redox reactions at electrodes on either side of the membrane stack. RED was originally envisioned as a method to capture energy derived from natural mixing processes, such as at estuaries where river water mixes freely with seawater.[11−13] However, synthetic electrolytes, such as ammonium bicarbonate (AmB), also can be used to capture energy from mixing processes.[14−19] AmB is easily distilled at low temperatures (40−60 °C), allowing an AmB−RED system to easily be coupled with a low grade waste heat driven distillation column for onsite regeneration of low concentration (LC) and high concentration (HC) salt solutions. A combined RED−distillation system creates a "closed loop" process, limiting the volume of solutions needed and the overall system size. The use of synthetic thermolytic solutions may also avoid some of the disadvantages with natural waters, such as the need for energy intensive pretreatment processes,[14] fixed solution salt concentrations, membrane fouling,[20] and geographic constraints relative to the availability of the source waters. There is also the potential to produce and harvest hydrogen gas, as chlorine evolution is no longer an issue. With the growing need to develop innovative solutions for industrial waste heat and waste acid recovery, an AmB−RED system could be an effective electrochemical method to neutralize acid and recover waste heat as either electricity or

hydrogen. This may be most possible at steel, iron, and petroleum industries, as there is typically an excess of both waste heat and waste acid solutions

The objectives of this study were to develop a new method to treat a low pH waste stream (acid) and to advance the performance of the RED system for capturing waste heat energy. The efficiency and performance of this waste acid disposal process were evaluated by varying stack and catholyte flow rates and using a 2-D transport model to identify the relative contributions of different ion transport mechanisms (electromigration, diffusion, and reaction) to acid neutralization. To study the electrochemical effect of using an acidic catholyte, the RED whole cell and anode and cathode performances were characterized using galvanostatic polarization curves with acidic, basic, and neutral electrolyte solutions (AmB). AmB was used in place of water in the electrolyte chambers because it also served as the RED stack solution. *In situ* hydrogen generation rates were measured and reported as a function of the RED stack flow rates.

■ MATERIALS AND METHODS

Reverse Electrodialysis Stack. The RED stack was a commercially available electrodialysis stack (PCcell, Heusweiler Germany) containing 20 cell pairs (41 membranes) each 0.5 mm thick. This unit had a total active membrane area of 0.87 m^2 and a projected surface area of 207 cm^2. The electrolyte rinse solutions (80 mL) were recycled through the anode and cathode chambers during all tests. Electrodes consisted of platinum/iridium (Pt/Ir) coatings on titanium electrodes and had projected areas of 207 cm^2. The HC solution was 1.4 M ammonium bicarbonate (AmB), and the LC was 5 mM AmB. The HC entered near to the cathode, and the LC entered near the anode (Figure 1). The HC and LC solutions (each 10 L) were recycled in a closed loop during batch (energy extraction) experiments for either 15 min or 1 h. During electrochemical polarization curves, the LC solutions were not recycled to ensure the stack ohmic resistance was constant.

Performance Data. Galvanostatic polarization was performed with a multi-channel potentiostat (model 1470E, Solartron Analytical,

Figure 1. Ammonium bicarbonate reverse electrodialysis (RED) stack with simultaneous hydrogen production and waste acid neutralization displayed at the cathode. RED mixed solutions (exit) are sent to a distillation column for regeneration. Dominate ion (ammonium, bicarbonate, and protons) flux directions are indicated by arrows.

Hampshire, England), with current scanned from 0 to 300 mA at 1 mA sec^{-1}. Ag/AgCl reference electrodes (BASi, West Lafayette, IN), placed on either side of the stack in the anolyte and catholyte, were used to record the stack, anode, and cathode individual potentials. Each electrochemical test was repeated between five and ten times to ensure reproducibility. The whole cell power was calculated by multiplying the current by the whole cell voltage $P_{cell} = I_{cell} U_{cell}$, and stack power was calculated through multiplying the current by the stacks voltage $P_{stack} = I_{cell} U_{stack}$. Power consumption due the electrode overpotential was calculating by taking the difference between the P_{cell} and P_{stack}.

Acid Neutralization. To evaluate the effect the stack flow had on the rate of acid neutralization, the RED stack was operated for 15 min at different stack flow rates of 100, 200, 400, or 600 mL min^{-1}, while the electrolyte rinse chamber flow rates were fixed at 150 mL min^{-1}. During the test, the stack was maintained at a fixed external resistance (10 Ω), and the voltage across the resistor was measured every second. The catholyte solution contained 0.01 M HCl (Sigma-Aldrich, St. Louis MO) (pH ∼ 2.0), and the anolyte contained 1.4 M AmB. The rate of neutralization was calculated as

$$r_n = \frac{-\log([H_{out}^+][H_{in}^+])}{t} \tag{1}$$

where $[H_{out}^+]$ is the concentration of protons in the catholyte at the end of testing, $[H_{in}^+]$ is the initial concentration of protons in the catholyte, and t is the duration of the experiment. The electrochemical efficiency for acid neutralization, which accounted for the acid neutralization process that occurred through the consumption of protons at the cathode ($2H^+ + 2e^- \rightarrow H_2$), was calculated using

$$\eta_{elec} = vF \frac{([H^+]_{in} - [H^+]_{out})}{(\int_{t=t}^{t=0} i dt)} \tag{2}$$

where v is the volume of acid neutralized, F is Faraday's constant (96485 C mol^{-1}), and i is current (A). The effect of the catholyte flow rate was investigated with the stack maintained at 400 mL min^{-1}, and the electrolyte flow rate was set to 10, 50, 100, or 150 mL min^{-1}.

Hydrogen Production Measurements. During batch tests, all solutions were recycled in a closed loop. The hydrogen produced over the complete batch cycle was measured by sampling the headspace of the electrolyte rinse bottle. The composition of gas sample was analyzed for H$_2$, N$_2$, and CO$_2$ using a gas chromatograph (GC, model 310 SRI Instruments argon carrier gas, NV), and the gas volume was calculated using the headspace volume. The hydrogen recovery was calculated through comparing the measured hydrogen produced to the theoretically hydrogen produced based on the measured current, as

$$r_{H_2} = \frac{(n_p F) n_{H_2}}{(\int_{t=t}^{t=0} i dt)} \tag{3}$$

where n_{H_2} is the moles of hydrogen recovered in the headspace, and n_p = 2 is the moles of charge required per mole of product (H$_2$) produced.

Transport Modeling. The transport of protons from the acidic catholyte to the adjacent HC solutions occurs due to diffusion, electromigration, and convection. In order to distinguish these transport mechanisms, a model of the end membrane, HC chamber, and catholyte was generated based on the Nernst−Planck equation

$$N_i = -D_i \nabla c_i - z_i u_{m,i} F c_i \nabla \varphi_e + c_i u \tag{4}$$

where N_i is the total molar flux due to diffusion, migration, and convection. D_i is the diffusivity of the charge ion, c_i is the concentration, z_i is the species charge number, $u_{m,i}$ is the species mobility, ϕ_e the electrolyte potential, and u is the fluid velocity. Fluid velocities were set at the inlets, with values based on those used in the experiments. Constant voltage boundary conditions were set, consistent with the voltage across one membrane, as given by the Nernst equation
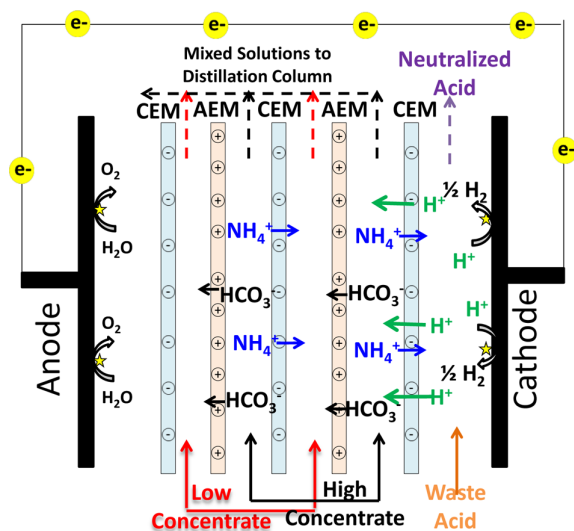
$$\varphi_m = \frac{RT}{F}\ln\left(\frac{a_{i,m}}{a_{i,e}}\right) \tag{5}$$

where $a_{i,m}$ is the activity of protons in the membrane, and $a_{i,e}$ is the activity of protons in the electrolyte. The total electrolyte current densities was then obtained through Faradays law

$$i_e = F\sum_n^{i=1} z_i(-D_i\nabla c_i - z_i u_{m,i} Fc_i \nabla \varphi_e) \tag{6}$$

where n represents the number of discretized steps.

■ RESULTS AND DISCUSSION

Waste Acid Neutralization Performance. Stack and catholyte flow rate (FR) both influenced the rate of acid neutralization. As the stack flow rate increased 6× from 100 to 600 mL min^{-1}, the rate of neutralization increased nearly 50× (from 0.06 ± 0.04 to 3.0 ± 0.32 pH units min^{-1} m^{-2}) (Figure 2). Increasing the catholyte flow rates by 1.5× from 10 to 150
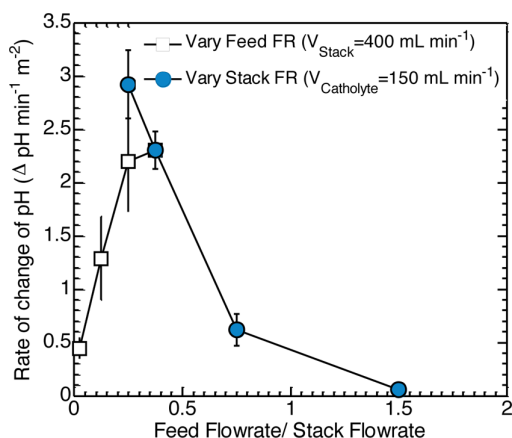

Figure 2. Catholyte neutralization rate as a function of ratio of the stack to catholyte flow rate.

mL min^{-1} resulted in an ~475% increase in the rate of neutralization (from 0.4 ± 0.09 to 2.3 ± 0.17 pH units min^{-1} m^{-2}).

The increase in the rate of acid neutralization at higher stack flow rates was due to the improved stack performance (power and current) (Figure S1, Supporting Information). An increase in the electrical current enhanced the ionic current, and the rate of ammonium transport into the catholyte. Furthermore, increasing the stack flow rate helped to maintain a high proton gradient across the end membrane, which promoted greater proton diffusion out of the catholyte (Figures S2 and S3, Supporting Information). Higher stack flow rates also increased hydrogen generation rates, which further contributed to acid neutralization (i.e., $2H^+ + 2e^- \rightarrow H_2$). The portion of acid neutralized through the hydrogen evolution reaction was expected to be low, as the neutralization efficiency (a measure of the protons used for hydrogen evolution) after only 15 min was significantly over 100% (e.g., 300% at 150 mL min^{-1}), indicating other methods of neutralization dominated (Figure S4, Supporting Information). The drop in neutralization efficiency during long-term testing (1 h) was observed because all the acid was neutralized early in the batch cycle. A high catholyte flow rate was important for removing the produced H$_2$ from the cathode surface and into the headspace. By

accumulating hydrogen at the cathode, the overall catalyst area decreases, which can reduce the rate of gas evolution.

Transport Modeling. Acid neutralization in the RED waste acid disposal system occurred by three different mechanisms: (1) transport of protons from the catholyte into the stack by diffusion, (2) transport of ammonium from the stack into the catholyte to maintain electroneutrality, and (3) proton removal through the production of hydrogen gas. The amount of protons consumed at the cathode and ammonium transported due to electromigration can be estimated using the experimentally obtained current data, using the assumption that for 1 mol e− transported through the circuit, 1 mol of NH$_4^+$ will be transported into the catholyte, and 1/2 mol of H$_2$ is produced. Protons transported across the membrane due to diffusion can be calculated based on a 2-D transport model, where the chemical flux ($j = -DdC/dx$) is calculated along the length of the catholyte channel (Figure S5, Supporting Information).

Simulations of the ion transport in the RED waste acid disposal system showed that the majority of acid neutralization in the catholyte occurred primarily by diffusion of protons (60 ± 5%) into the stack solution, followed by electromigration of ammonium ions (37 ± 4%). Only a small fraction (~4%) of the acid neutralization took place through proton consumption at the cathode (Figure 3). This was found in all cases irrespective
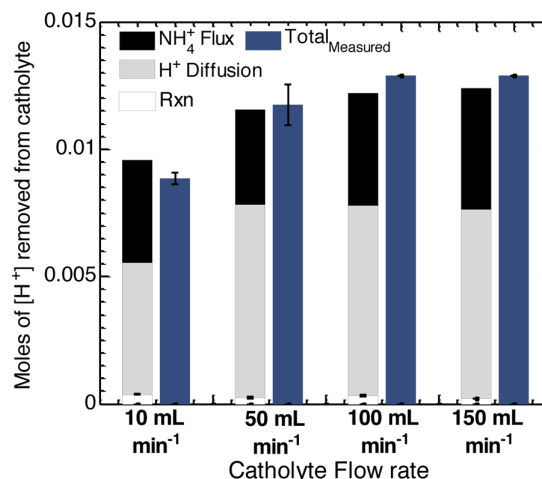

Figure 3. Protons transport mechanism during testing where the catholyte flow rate was varied, and the stack flow rate was fixed at 400 mL min^{-1}.

of the stack and catholyte flow rates (Figure S6, Supporting Information). This result is consistent with the estimate made on the basis of neutralization efficiencies (Figure S4, Supporting Information). The rate of acid neutralization in the RED system was therefore primarily dependent on the existence of a large pH gradient across the end membrane to promote diffusion and electrical current that promoted electromigration. Increasing the acid concentration, while maintaining the membrane surface area and catholyte flow rate, would result in a decrease in the rate of neutralization. Thus, in order to ensure sufficient rates of neutralization, the membrane surface area or catholyte flow rate would need to be increased.

Reverse Electrodialysis System Performance with Acidic and Basic Catholytes. Using a basic (NaOH) anolyte

with the AmB catholyte increased the overall power production by 50% (from 0.06 ± 0.001 W to 0.09 ± 0.004 W), compared to tests with AmB as both anolyte and catholyte. Using an acidic (HCl) catholyte with an AmB anolyte increased power by 66% (0.06 ± 0.001 W to 0.1 ± 0.005 W), when compared to a neutral pH AmB electrolyte (anolyte and catholyte) (Figure 4). Using a basic anolyte and an acidic catholyte produced the
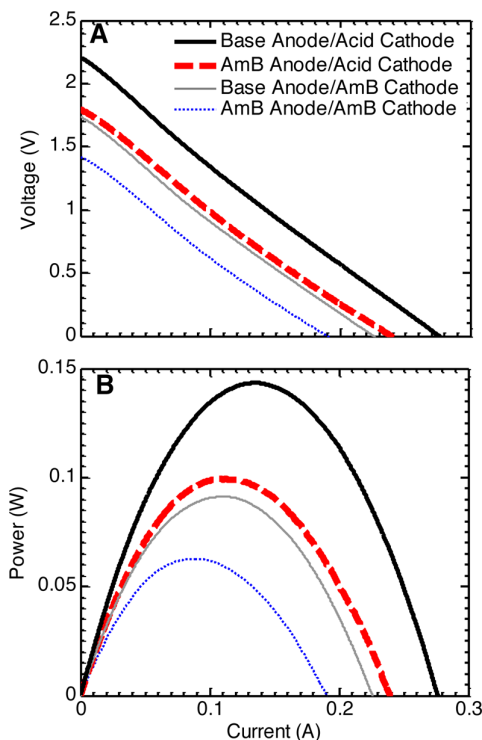

Figure 4. System whole cell (a) polarization curve and (b) power density data with dissimilar electrolytes (AmB, Acid, and base). Stack flow rate was 600 mL min^{-1} in all tests.

greatest increase in power of ~130% (0.06 ± 0.001 to 0.14 ± 0.004 W), compared with AmB in both electrode chambers. In all tests the stack power density remained constant (0.3 ± 0.004 W), indicating that the increased performance was due solely to the improved electrode kinetics for hydrogen (cathode) and oxygen (anode) evolution. Reducing the power drop between the stack and whole cell is essential for performance, efficiency, and cost. AmB was used as the neutral pH control because this minimized the crossover of species between the stack and electrolyte solutions.

The improved performance obtained using the acid and base solutions is consistent with improved thermodynamics predicted for the water splitting reaction. On the basis of the Nernst equation, there is an intrinsic relationship between the potential at which hydrogen and oxygen is evolved and the solution pH ($E_{H+/H_2} = E^0 - 0.059 \times$ pH), where E^0 is the standard potential for hydrogen or oxygen generation. Shifting the pH can aid in reducing the energy consumed to initiate the reaction (hydrogen or oxygen evolution) (Figure S7, Supporting Information). The onset potential for O_2 evolution decreased by 374 mV with the basic anolyte, when compared to AmB. Likewise, the onset potential for H_2 evolution increased by 389 mV with an acidic catholyte, when compared to AmB

(Figure 5). These results also highlight the benefits of using dissimilar electrolytes in an electrolysis cell to mitigate
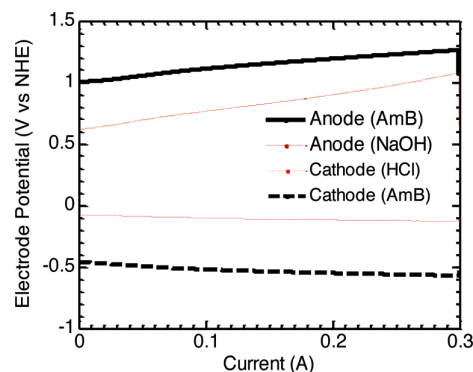

Figure 5. Individual electrode potentials with AmB anolytes, basic anolyte, acidic catholyte, and AmB catholyte with the stack operated at 600 mL min^{-1}.

electrode overpotential, while avoiding direct crossover of products from the anolyte to catholyte due to the presence of the membrane stack.

Hydrogen Energy Production. The hydrogen production rate increased linearly with the stack flow rate ($R^2 = 98 \pm 1\%$; $P = 0.01 \pm 0.006$) (Figure 6). The maximum hydrogen
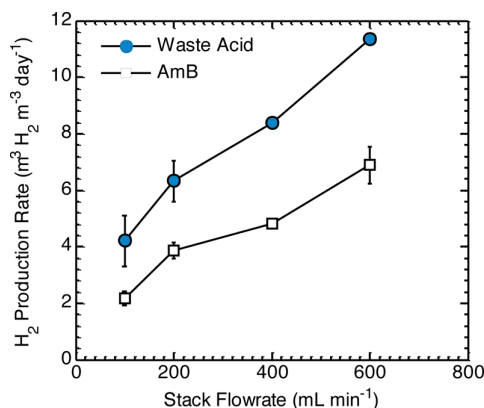

Figure 6. Measured hydrogen production rate using the waste acid or AmB catholyte.

production rate for the synthetic waste acid (WA) catholyte approached 8.7 ± 0.1 m^3 H$_2$ m^{-3} day^{-1} at 600 mL min^{-1}, which was 65% greater than that produced with AmB (5.3 ± 0.5 m^3 H$_2$ m^{-3} day^{-1}). With high flow rates the whole cell power and current both increase, which results in elevated hydrogen production rates. The peak power increased by >250% (0.016 to 0.061 W m^{-2}) with an AmB catholyte and by >150% (0.033 to 0.083 W m^{-2}) with an WA catholyte as the stack flow rate was increased from 100 mL min^{-1} to 600 mL min^{-1} (Figure S1, Supporting Information). For all flow rates, the WA catholyte produced between 60−90% more hydrogen than AmB, which was consistent with the increase in whole cell power by 30−90%.

A reduction in the rate of hydrogen production at the low flow rates was due to a loss of hydrogen gas from the catholyte chamber into the stack. Cathodic recovery of H$_2$ gas decreased from $70.5 \pm 4\%$ to $40 \pm 10\%$ as the flow rate was reduced from

600 to 100 mL min^{-1} (Figure 7). A higher liquid flow rate increases the shear at the electrode surface, which would
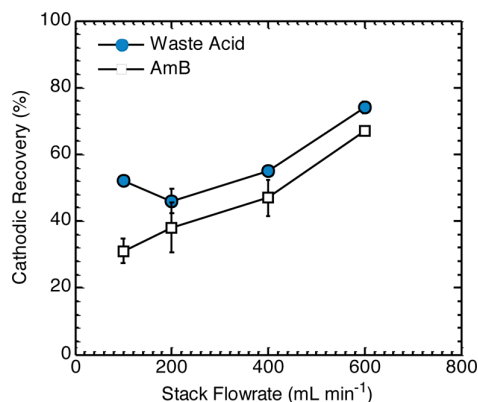

Figure 7. Cathodic recovery of hydrogen gas using RED with waste acid or AmB catholytes.

improve hydrogen gas transfer from the cathode surface. A higher flow rate also improves gas transport from the reactor and into the bottle headspace, which could reduce the loss of hydrogen due to crossover into the membrane stack. High flow rates require more pumping energy, and therefore, developments to mitigate hydrogen losses from the catholyte at low flow rates could improve the overall energy balance.

One major disadvantage to using AmB as a catholyte is the loss of CO_2 from the solution. When an acid solution was used in the catholyte, the product gas was nearly all H_2, but when AmB was used as the catholyte the gas was ~80% CO_2 (Figure S8, Supporting Information). CO_2 if captured can be recycled and used to regenerate stack solutions, but high purity hydrogen is preferable if hydrogen is to be sold or used within fuel cells to generate electricity. It is projected here that the mixed gases could still be valuable, as synthetic gases (syngas) are already used at steel, iron, and petroleum industries for electricity production through combustion or to make valuable products such as synthetic petroleum. Separation of the mixed gases would likely not be a viable method to recovery pure hydrogen as it is too energy intensive.

CONCLUSIONS

AmB−RED systems provide opportunities for simultaneous renewable hydrogen production, waste heat conversion, and waste acid neutralization. An AmB−RED system was shown to be effective at neutralizing the waste acid stream, with a rate of neutralization that could be increased nearly 50× by increasing the stack flow rate 6×. Acid neutralization occurred primarily due to diffusion of protons ($60 \pm 5\%$) and electromigration of ammonium from the stack into the catholyte ($37 \pm 4\%$). Energy recovery through hydrogen increased by as much as 65% by using waste acid as the catholyte, compared to neutral pH AmB solutions.

ASSOCIATED CONTENT

Ⓢ Supporting Information

Further electrochemical and modeling analyses. This material is available free of charge via the Internet at http://pubs.acs.org.

AUTHOR INFORMATION

Corresponding Author

*E-mail: blogan@psu.edu. Phone: +1-814-863-7908.

Notes

The authors declare no competing financial interest.

REFERENCES

(1) Energy Recovery from Waste. U.S. Environmental Protection Agency. http://www.epa.gov/osw/nonhaz/municipal/wte/.

(2) Zhu, X.; Hatzell, M. C.; Cusick, R. D.; Logan, B. E. Microbial reverse-electrodialysis chemical-production cell for acid and alkali production. *Electrochem. Commun.* **2013**, *31* (1388−2481), 52−55.

(3) German, M.; SenGupta, A. K.; Greenleaf, J. Hydrogen ion (H+) in waste acid as a driver for environmentally sustainable processes: opportunities and challenges. *Environ. Sci. Technol.* **2013**, *47* (5), 2145−2150.

(4) Sarkar, S.; SenGupta, A. K.; Greenleaf, J. E.; El-Moselhy, M. Energy recovery from acid−base neutralization process through pH-sensitive polymeric ion exchangers. *Ind. Eng. Chem. Res.* **2011**, *50* (21), 12293−12298.

(5) Zhu, X.; Yang, W.; Hatzell, M.; Logan, B. E. Energy recovery from solutions with different salinities based on swelling and shrinking of hydrogels. *Environ. Sci. Technol.* **2014**, *48* (12), 7157−7163.

(6) Post, J.; Goeting, C.; Valk, J.; Goinga, S.; Veerman, J.; Hamelers, H.; Hack, P. Towards implementation of reverse electrodialysis for power generation from salinity gradients. *Desalin. Water Treat.* **2010**, *16* (1−3), 182−193.

(7) Veerman, J.; Saakes, M.; Metz, S.; Harmsen, G. Reverse electrodialysis: Evaluation of suitable electrode systems. *J. Appl. Electrochem.* **2010**, *40* (8), 1461−1474.

(8) Veerman, J.; Saakes, M.; Metz, S.; Harmsen, G. Reverse electrodialysis: Performance of a stack with 50 cells on the mixing of sea and river water. *J. Membr. Sci.* **2009**, *327* (1−2), 136−144.

(9) Veerman, J.; Post, J.; Saakes, M.; Metz, S.; Harmsen, G. Reducing power losses caused by ionic shortcut currents in reverse electro-dialysis stacks by a validated model. *J. Membr. Sci.* **2008**, *310* (1), 418−430.

(10) Post, J. W.; Veerman, J.; Hamelers, H. V. M; Euverink, G. J. W.; Metz, S. J.; Nymeijer, K.; Buisman, C. J. N. Salinity-gradient power: Evaluation of pressure-retarded osmosis and reverse electrodialysis. *J. Membr. Sci.* **2007**, *288* (1−2), 218−230.

(11) Weinstein, J. N.; Leitz, F. B. Electric power from differences in salinity: The dialytic battery. *Science* **1976**, *191* (4227), 557.

(12) Veerman, J.; Saakes, M.; Metz, S. J.; Harmsen, G. J. Electrical power from sea and river water by reverse electrodialysis: A first step from the laboratory to a real power plant. *Environ. Sci. Technol.* **2010**, *44* (23), 9207−9212.

(13) Ramon, G. Z.; Feinberg, B. J.; Hoek, E. M. V. Membrane-based production of salinity-gradient power. *Energy Environ. Sci.* **2011**, *4* (11), 4423−4434.

(14) Logan, B. E.; Elimelech, M. Membrane-based processes for sustainable power generation using water. *Nature* **2012**, *488* (7411), 313−319.

(15) McGinnis, R. L.; McCutcheon, J. R.; Elimelech, M. A novel ammonia−carbon dioxide osmotic heat engine for power generation. *J. Membr. Sci.* **2007**, *305* (1), 13−19.

(16) McCutcheon, J. R.; McGinnis, R. L.; Elimelech, M. A novel ammonia−carbon dioxide forward (direct) osmosis desalination process. *Desalination* **2005**, *174* (1), 1−11.

(17) Hatzell, M. C.; Logan, B. E. Evaluation of flow fields on bubble removal and system performance in an ammonium bicarbonate reverse electrodialysis stack. *J. Membr. Sci.* **2013**, *446*, 449−455.

(18) Hatzell, M. C.; Cusick, R. D.; Ivanov, I.; Zhu, X.; Logan, B. E. Comparison of hydrogen production and electrical power generation for energy capture in closed-loop ammonium bicarbonate reverse electrodialysis systems. *Phys. Chem. Chem. Phys.* **2014**, *16* (4), 1632−1638.

(19) Cusick, R. D.; Kim, Y.; Logan, B. E. Energy capture from thermolytic solutions in microbial reverse-electrodialysis cells. *Science* **2012**, *335* (6075), 1474−1477.

(20) Vermaas, D. A.; Kunteng, D.; Saakes, M.; Nijmeijer, K. Fouling in reverse electrodialysis under natural conditions. *Water Res.* **2013**, *47* (3), 1289−1298.